Structure of a Human *S*-Adenosylmethionine Decarboxylase Self-Processing Ester Intermediate and Mechanism of Putrescine Stimulation of Processing As Revealed by the H243A Mutant[†,‡]

Jennifer L. Ekstrom,[§] W. David Tolbert,[§] Haishan Xiong,[||] Anthony E. Pegg,[||] and Steven E. Ealick*[,§]

Department of Chemistry and Chemical Biology, Cornell University, Ithaca, New York 14853-1301, and Departments of Cellular and Molecular Physiology and of Pharmacology, Milton S. Hershey Medical Center, Pennsylvania State University College of Medicine, Hershey, Pennsylvania 17033

Received April 11, 2001; Revised Manuscript Received June 5, 2001

ABSTRACT: *S*-Adenosylmethionine decarboxylase (AdoMetDC) is synthesized as a proenzyme that cleaves itself in a putrescine-stimulated reaction via an N→O acyl shift and β-elimination to produce an active enzyme with a catalytically essential pyruvoyl residue at the new N-terminus. N→O acyl shifts initiate the self-processing of other proteins such as inteins and amidohydrolases, but their mechanisms in such proteins are not well understood. We have solved the crystal structure of the H243A mutant of AdoMetDC to 1.5 Å resolution. The mutant protein is trapped in the ester form, providing clear evidence for the structure of the ester intermediate in the processing of pyruvoyl enzymes. In addition, a putrescine molecule is bound in a charged region within the β-sandwich, and cross-links the two β-sheets through hydrogen bonds to several acidic residues and ordered water molecules. The high-resolution structure provides insight into the mechanism for the self-processing reaction and provides evidence for the mechanism for simulation of the self-processing reaction by putrescine. Studies of the effects of putrescine or 4-aminobutanol on the processing of mutant AdoMetDC proenzymes are consistent with a model in which a single activator molecule interacts with buried Asp174, Glu178, and Glu256, leading to an alteration in the position of Glu11, resulting in stimulation of self-processing.

S-Adenosylmethionine decarboxylase (AdoMetDC)[1] belongs to the small family of pyruvoyl enzymes whose catalytic reactions require a covalently bound pyruvoyl group that is produced via an autocatalytic intramolecular cleavage reaction (*1*, *2*). The structure of the fully processed human AdoMetDC has been reported at 2.25 Å resolution (*3*), and several complexes of AdoMetDC with substrate analogues and inhibitors have also been determined (*4*). These structures show that the AdoMetDC monomer adopts a novel four-layer $\alpha\beta\beta\alpha$ sandwich fold (*3*) and provide details of the active site. The structures of two other pyruvoyl enzymes, *Lactobacillus 30a* histidine decarboxylase (HisDC) (*5*) and *E. coli* aspartate decarboxylase (AspDC) (*6*), have also been determined. Remarkably, these three pyruvoyl-dependent decarboxylases show no structural homology to one another.

Human AdoMetDC is synthesized as a 38.3 kDa proenzyme (π chain) that undergoes self-cleavage at the Glu67−Ser68 peptide bond, generating two chains, β and α, of molecular mass 7.7 and 30.6 kDa, respectively (β is the N-terminal chain and α is the C-terminal chain by convention). The active AdoMetDC is isolated as a 76.6 kDa $(\alpha\beta)_2$ dimer (*1*). The self-cleavage reaction occurs through nonhydrolytic serinolysis, in which the side chain hydroxyl group of Ser68 supplies its oxygen to form the C-terminus of the β-chain, while the remainder of the Ser residue is converted to ammonia and the pyruvoyl group that blocks the N-terminus of the α-chain (Scheme 1). AdoMetDC, HisDC (*5*), and AspDC (*6*) appear to utilize similar mechanisms for self-cleavage. However, the only structural evidence for the self-cleavage reaction comes from AspDC in which one of the four subunits is unprocessed (*6*). The analysis of this structure is complicated by disorder in the region of the putative ester bond.

Studies of the AdoMetDC processing reaction by site-directed mutagenesis have identified several mutants that fail to process or process very slowly. These include mutations at Ser68 (*7*) and mutations at the conserved residues His243 and Ser229 (*8*). Mutant S229A failed to process, and the resulting proenzyme resembled the S68A mutant, suggesting that the hydroxyl group of residue 229 is required for the processing reaction. Mutant H243A cleaved very slowly, but

[†] This work was supported by the Biomedical Research Resource Program (RR-01646) and the National Cancer Institute (Grant CA-18138 to A.E.P.) of the National Institutes of Health. S.E.E. is also indebted to the W. M. Keck Foundation and the Lucille P. Markey Charitable Trust.

[‡] The coordinates of the H243A AdoMetDC structure have been deposited in the Protein Data Bank under accession number 1JL0.

* To whom correspondence should be addressed at the Department of Chemistry and Chemical Biology, Cornell University, Ithaca, NY 14850. Telephone: (607) 255-7961. Fax: (607) 255-1227. E-mail: see3@cornell.edu.

[§] Cornell University.

[||] Pennsylvania State University College of Medicine.

[1] Abbreviations: AdoMetDC, *S*-adenosylmethionine decarboxylase; HisDC, histidine decarboxylase; AspDC, aspartate decarboxylase; *E. coli*, *Escherichia coli*; AdoMet, *S*-adenosylmethionine; GABA, γ-aminobutyric acid; HPLC, high-performance liquid chromatography; bp, base pair(s); PCR, polymerase chain reaction; TNT, T7-coupled transcription and translation kit; Tris, tris(hydroxymethyl)aminomethane; PEG, poly(ethylene glycol); CCD, charge-coupled device.

10.1021/bi010736o CCC: $20.00
Published on Web 07/21/2001

Scheme 1

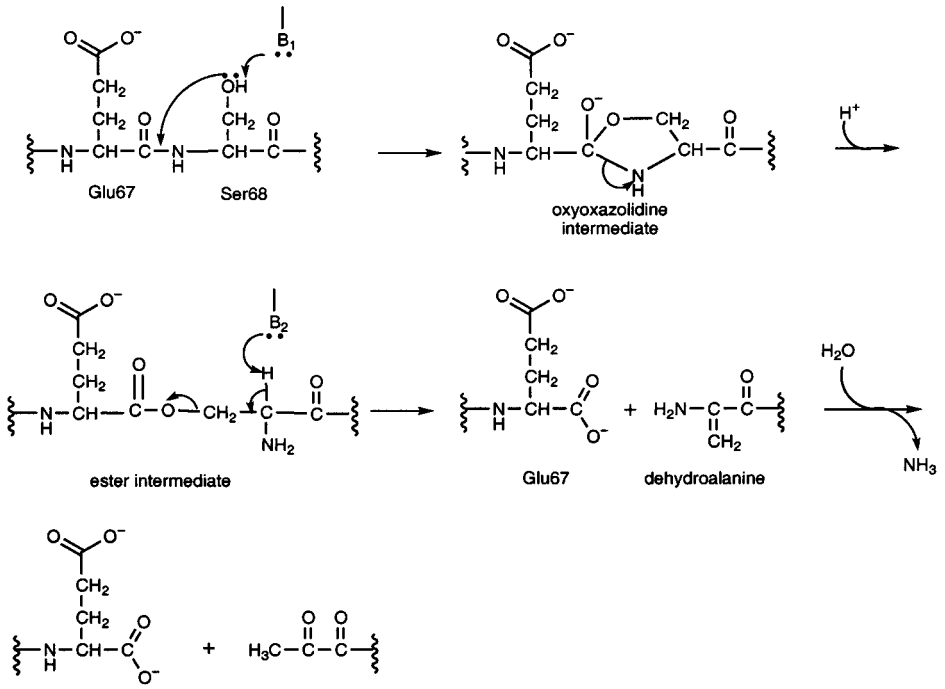

the proenzyme from this mutant was readily split by hydroxylamine, generating an α-subunit with an N-terminal serine formed by Ser68. This result suggests that the N→O acyl shift needed for ester formation occurs normally in the H243A mutant but that the next step, which is a β-elimination reaction leading to the two subunits, does not occur. Therefore, H243A mutant AdoMetDC was selected for structural analysis.

The rate of the intramolecular self-cleavage reaction in human AdoMetDC is accelerated by the diamine putrescine (*9*). The $t_{1/2}$ of the processing reaction shortens from 2 h to 15 min upon the addition of millimolar putrescine (*10*). Putrescine also enhances the enzymatic activity of the mature protein; the addition of submillimolar putrescine lowers the K_m for the substrate 4-fold at pH 6.8 (*11*). This dual allosteric activation provides a mechanism for regulating polyamine levels, since both the amount of processed AdoMetDC and its enzymatic activity are enhanced by the availability of putrescine for the downstream reactions. The structure of native AdoMetDC together with site-directed mutagenesis data suggested that an unusual constellation of negatively charged residues between the β-sheets, well-removed from the active site, was the binding site for the positively charged putrescine molecule (*3*).

Putrescine stimulation, however, is not universal among AdoMetDCs. More than 30 AdoMetDC cDNAs and derived amino acid sequences are now available; these fall into 2 classes. Class 1 (microbial) enzymes resemble the Mg^{2+}-activated *Escherichia coli* AdoMetDC (*12*), with a tetrameric $(\alpha\beta)_4$ quaternary structure, and have the sequence -DK∼SHI- or -E∼SH(L/I/V)- at the cleavage site (*1, 12*). Class 2 enzymes (including those from mammals, plants, protozoan, and fungi) resemble the human AdoMetDC, with a dimeric $(\alpha\beta)_2$ quaternary structure, and have the sequence -(L/V)L-(S/T/N)E∼SS(L/M/E)(F/M)(F/I/V)- at the cleavage site (*1, 9*). There is very little similarity between the primary amino acid sequences of the Class 1 and Class 2 AdoMetDCs. Putrescine enhances the enzymatic activity of some Class 2 AdoMetDCs (*13*) such as mammals, fungi (*14*), and trypanosomes (*15, 16*) but not others, such as plants (*7*).

In addition to the pyruvoyl-dependent decarboxylases, a number of other self-activating proteins have been recently shown to undergo analogous covalent backbone rearrangements without external catalysts. Prominent examples include inteins, the hedgehog protein, amidohydrolases, and the yeast nucleoporin Nup145p (*17, 18*). The various self-processing reactions of these proteins all involve an initial N→O (or N→S) acyl shift, converting a specific peptide bond into a more reactive ester (or thioester) intermediate. The precise mechanisms of N→O acyl shifts in these proteins are poorly understood, due to the relatively sparse structural data on precursor species. We present here the 1.5 Å resolution crystal structure of the H243A mutant of human AdoMetDC. This structure contains a trapped ester intermediate of the self-processing reaction and suggests roles of key residues in various steps of the self-cleavage reaction.

EXPERIMENTAL PROCEDURES

Materials. The T7-coupled transcription and translation (TNT) kit, Wizard Miniprep kit, and RNAsin were purchased from Promega (Madison, WI). The Chameleon double-stranded site-directed mutagenesis kit and XL1-Blue *E. coli* competent cells were purchased from Stratagene (La Jolla, CA). Ligation Express kit was a product of Clontech (Palo Alto, CA). The restriction enzymes used were from Gibco BRL (Gaithersburg, MD), Promega, and New England BioLabs (Beverly, MA). Sequenase V 2.0 DNA polymerase was from Amersham (Arlington Heights, IL). Human AdoMetDC cDNA was subcloned into the pGEM3Zf- vector to form pCM9 (*19*). [^{14}COOH]AdoMet was from Amersham. Unlabeled AdoMet, 1,3-diaminopropane, putrescine, cadaverine, 1,6-diaminohexane, 1,7-diaminoheptane, 1,8-diaminooctane, imidazole, GABA, 4-aminobutanol, 1,4-butanediol, tetramethyl-1,4-butanediamine, tetramethyl-

Table 1: X-ray Data Processing and Structural Refinement Statistics

	99−1.50 Å	1.55−1.50 Å
data collection statistics		
completeness (%)	98.8	99.5
redundancy	4.0	3.9
$I/\sigma_{(I)}$	17.9	4.6
R_{merge}	0.069	0.275
refinement statistics		
R/*R*-free	0.215/0.237	
rmsd bonds (Å)	0.006	
rmsd angles (deg)	1.32	

ammonium iodide, and Ponceau S solution were purchased from Aldrich (Milwaukee, WI) or from Sigma (St. Louis, MO). The 4-aminobutanol used was checked for contamination by putrescine by HPLC, and none was detected with a sensitivity of less than 0.05%. All other chemicals were from Fisher (Pittsburgh, PA).

Expression and Crystallization. The AdoMetDC H243A point mutant was prepared and inserted into a pQE30 plasmid for expression as described (*20*). *E. coli* JM109 cells containing this plasmid were grown at 37 °C in LB media with 100 μg/mL ampicillin, and induced after 2 h by the addition of 100 μg/mL isopropyl-1-thio-β-D-galactopyranoside. The cells were grown for 4 additional h, harvested, and lysed by sonication (*3*). The histidine-tagged enzyme was purified by metal-affinity chromatography as described previously (*3*). Crystals of the H243A mutant were grown by the hanging-drop method at 4 °C in 15% PEG 8K, 100 mM Tris-HCl, pH 8.0 (*3*), and reached their full size (0.4 × 0.7 mm) within 2−3 weeks. The mutant protein crystallized in the monoclinic space group $P2_1$ with unit-cell dimensions of $a = 74.76$ Å, $b = 55.99$ Å, $c = 90.21$ Å, and $\beta = 109.72°$ and one dimer in the asymmetric unit.

X-ray Data Collection and Processing. The crystals were frozen in liquid nitrogen in a cryoprotectant solution of 15% glycerol in 17% PEG 8K, 100 mM Tris, pH 8.0, and transferred to a gaseous N_2 stream as described previously (*3*). Diffraction data on the H243A crystal were measured at the Structural Biology Center beamline (Advanced Photon Source) using the SBC-1 3 × 3 mosaic CCD detector. The data were indexed and scaled to 1.5 Å using HKL2000 (*21*), with a resulting R_{merge} of 6%. The data processing statistics are presented in Table 1.

Structure Solution and Refinement. The structural solution and refinement were carried out using the CNS refinement package (*22*), using the 2.25 Å native human AdoMetDC structure (PDB 1JEN) as the starting model for molecular replacement. All reflections above 1σ in the range from 20 to 1.5 Å resolution were used in refinement except for a 10% randomly selected test set used for calculation of R_{free} (*23*). A flat bulk solvent model was used throughout the refinement. Several cycles of rigid body refinement, minimization, and simulated annealing were performed, and initial maps were calculated. A clear connection between Glu67 and Ser68 was apparent in the electron density (Figure 1). In addition, a strong, well-formed chain of electron density corresponding to the effector putrescine was observed within the hydrophilic intersheet cavity during the first cycle of water placement. Models of putrescine and of the ester linkage were created using the program SYBYL (*24*) and positioned within the density using the graphics program O (*25*). After additional refinement, multiple side chain positions were modeled as supported by the F_o-F_c and $2F_o-F_c$ difference maps. A recurring section of strong electron density observed at the entrance of the active site was identified and modeled as a molecule of the buffer Tris. CNS topology and parameter files for putrescine, Tris, and the ester linkage were created using the program XPLO2D (*26*). Alternate cycles of rebuilding, positional refinement, simulated annealing, *B*-factor refinement, and water placement were performed to reduce R_{free} iteratively to its final value of 23.7% ($R = 21.5\%$).

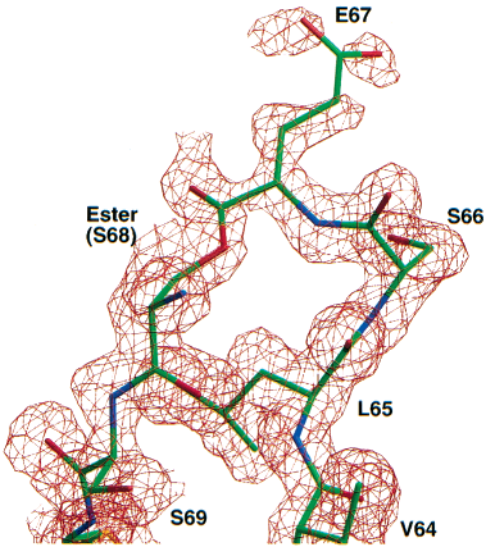

FIGURE 1: Model of the observed ester reaction intermediate with its corresponding electron density, contoured at 1σ. The model is generally well-resolved throughout this region, with most atomic *B*-factors between 7 and 15 Å^2.

The protein model was assessed using the program PROCHECK (*27*). The Ramachandran plot (*28*) showed 89.6% of the residues in the most favored region and 9.7% in the additional allowed region. Residue Gln300 of each monomer lies in the disallowed region, but has electron density that reappears in omit maps. Final refinement statistics and measures of model quality are presented in Table 1.

Mutagenesis and Plasmid Construction. Mutants E11Q, E178Q, E256Q, and D174N have been described previously (*7*, *11*, *29*). Additional point mutations were also made in the pCM9 vector using the Chameleon mutagenesis kit following manufacturer's recommendations. The primers used were as follows: D174E, 5′-CAAGGTTTGCTCTGGCTGACTG-3′; E11D, 5′-CTCCAGCAGCTTTGCGGTCCCTTCG-3′; E178D, 5′-CTCATCAGAATGTCCAAGGTTTG-3′; E256D, 5′-CTTAAGTTTGTGTCAAAGCTAAC-3′. Double mutants were generated using one of the following methods. For E11D/X (X = D174E, E178D, and E256D) double mutations, plasmids containing either D174E, E178D, or E256D mutations were digested with *Bgl*II and *Xba*I. The 950 bp digestion products were ligated to the vector plasmid containing the E11D mutation that had been digested with the same enzymes. For E256D/X (X = D174E and E178D) double mutations, PCR reactions were done using a T7 sense and E256D antisense primer set with vectors containing D174E (for E256D/D174E double mutation) or E178D (for E256D/E178D double mutation) as templates. The 900 bp PCR products were digested with *Csp*45I and *Afl*II, and the

755 bp digestion products were inserted into the pCM9 vector digested with the same enzymes. The complete coding sequences of all of the mutated AdoMetDC cDNA sequences were checked to confirm that the desired mutation was present and that no other mutations had occurred.

In Vitro Protein Synthesis and Processing Assay. Wild-type and mutant AdoMetDC proteins were synthesized in TNT reactions, and the processing assays were performed as described earlier (*7*), except that in some of the reactions putrescine analogues were added. The rate of the processing in the absence of putrescine complies with first-order reaction kinetics (*9*). The fractional rate of processing and affinity for activators was calculated (*7*) using KaleidaGraph (Abelbeck Software) to fit the processing data to the first-order equation.

AdoMetDC Activity Assay. The activity assay essentially followed the method described (*7*) using TNT-synthesized AdoMetDC enzymes by following the ability to convert [^{14}COOH]AdoMet to $^{14}CO_2$. Each assay contained 1.25 mM dithiothreitol, 50 mM sodium phosphate buffer, pH 6.8, and 9.6 μM [^{14}COOH]AdoMet (52 mCi/mol) in a total volume of 250 μL. Putrescine or 4-aminobutanol was added to some of the reactions to assess their effect on the enzymatic activity.

RESULTS

Structure of H243A AdoMetDC. The H243A mutant of AdoMetDC crystallizes in the space group $P2_1$ with unit-cell dimensions of $a = 74.76$ Å, $b = 55.99$ Å, $c = 90.21$ Å, and $\beta = 109.72°$. These crystals are similar to those of wild-type AdoMetDC and contain one $(\alpha\beta)_2$ dimer in the asymmetric unit. A ribbon diagram of the H243A dimer is depicted in Figure 2. The monomer fold consists of two layers of β-sheets sandwiched between two layers of $\alpha-$helices. The structure of the H243A mutant is largely identical to that of the fully processed protein (*3*), with three important differences.

The most obvious difference between the structures of the fully processed AdoMetDC and the H243A mutant is the presence of the ester bond between Glu67 and Ser68 in the mutant enzyme. Glu67 and Ser68 are connected by continuous electron density, but their C^α atoms are separated by 4.55 Å (Figure 1; for comparison, the $C^\alpha-C^\alpha$ distance in normal trans peptide bonds is 3.8 Å). The electron density and stereochemical constraints clearly indicate that these C^α atoms are linked by three heavy atoms, rather than two as would be expected for an amide linkage. Finally, the electron density adjacent to the C^α of Ser68 is consistent with the displaced α-amino group of the ester, showing a single heavy atom that makes hydrogen bonds to three well-ordered water molecules (W_A, W_C, and W_D) that are arranged tetrahedrally around the amino group nitrogen atom (Figure 3). These water molecules are anchored by a network of hydrogen bonds that connects the displaced α-amino group with residues on both layers of the β-sandwich. The ordered water W_C is hydrogen-bonded to the side chain oxygen of Ser229 and to the backbone carbonyl of Leu65. A water molecule corresponding to W_C is also present in the structure of the mature enzyme (*3*). The second ordered water, W_A, makes additional hydrogen bonds to Ser69 and two other waters. The third ordered water molecule, W_D, hydrogen-bonds to another ordered water, W_E, and possibly to the side chain of Cys82. W_E is also present in the mature enzyme and forms a hydrogen bond to the backbone carbonyl of Gly9 and to the $O^{\epsilon 1}$ of Glu11. By contrast, the intact serine side chain of the proenzyme does not fit into this density. Because biochemical experiments also support the presence of an ester intermediate in the H243A mutant (*8*), it is reasonable to conclude that an N→O acyl shift has occurred in the Glu67−Ser68 peptide bond of the H243A mutant, yielding a stable ester intermediate.

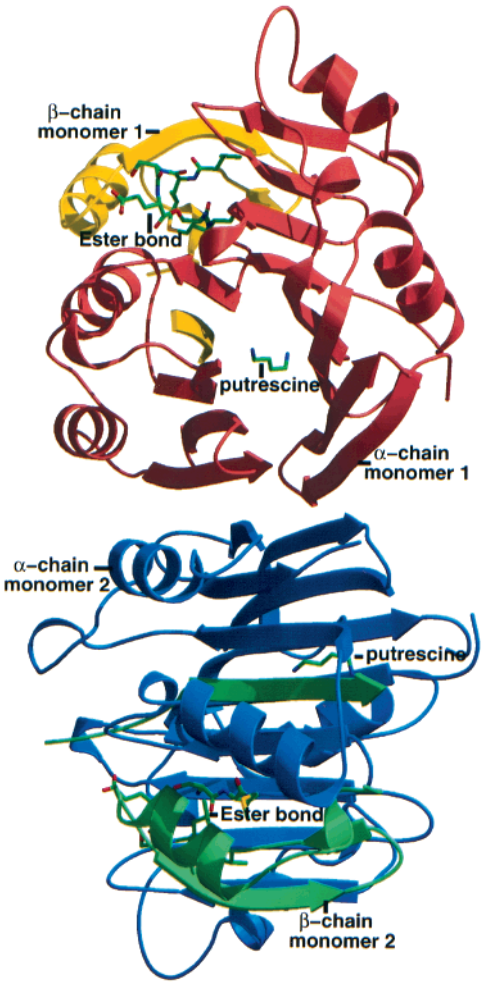

FIGURE 2: Ribbon diagram of the H243A mutant of AdoMetDC. The diagram illustrates the location of the ester bond and the putrescine binding site for each of the two monomers. Figures were prepared using BOBSCRIPT (*38*, *39*) and RASTER3D (*40*).

The second difference between the H243A structure and the previously reported fully processed structure is the presence of a well-defined chain of electron density corresponding to putrescine, the activator of both processing and catalytic activity, within the charged intersheet region. The general location of putrescine binding was predicted previously based on a highly unusual grouping of acidic residues buried within the otherwise hydrophobic β-sandwich core (*3*), and is supported by previous site-directed mutagenesis studies (*7*, *11*, *29*). A reanalysis of the electron density for the fully processed AdoMetDC indicates that putrescine was bound in that structure as well but was instead modeled as a series of ordered water molecules (*3*). The H243A crystal structure shows putrescine interacting with several conserved acidic and hydrophobic residues (Figure 4). The first amino

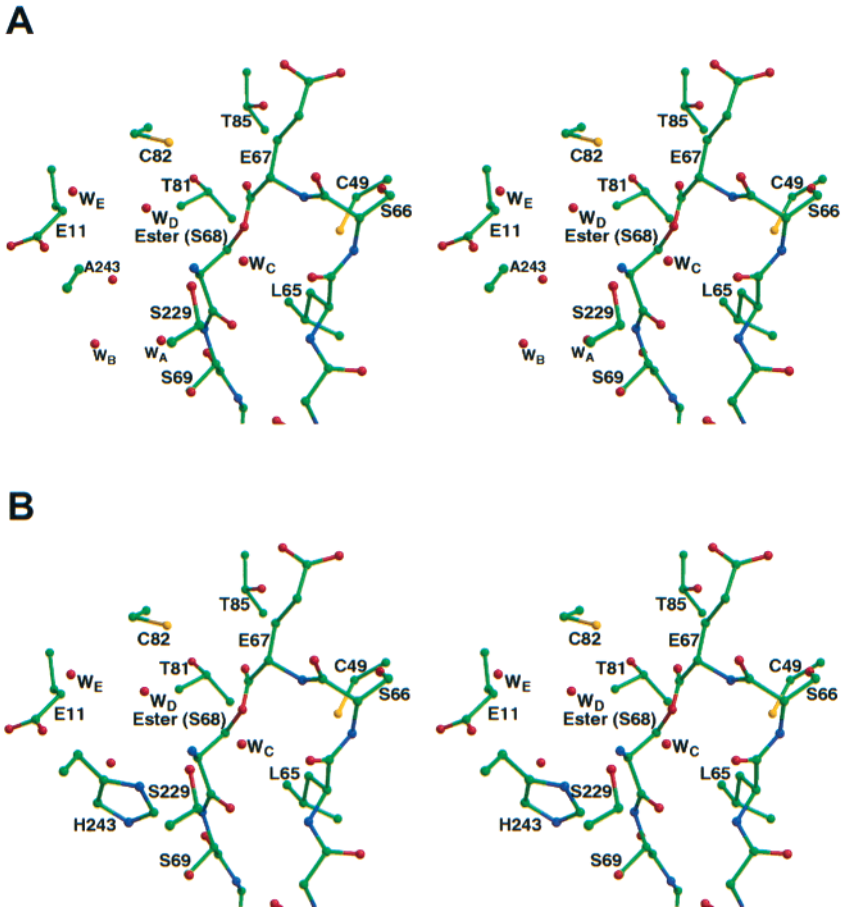

FIGURE 3: Stereoview of the ester linkage. (A) Three ordered waters (W_A, W_C, W_D) stabilize the displaced α-amino group of Ser68. The positions of W_A and W_B mimic the positions of the $N^{\delta 1}$ and $N^{\epsilon 2}$ atoms of His243. (B) Model of His243 generated by using the fully processed AdoMetDC coordinates to position the His243 side chain.

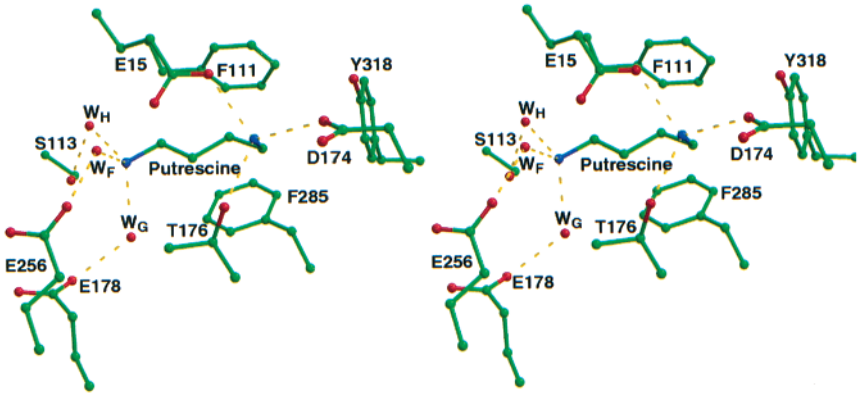

FIGURE 4: Stereoview of a ball-and-stick model of the putescine binding site. Key residues are shown with hydrogen bonds indicated by dashed lines.

group of putrescine hydrogen-bonds directly to the side chains of Glu15, Asp174, and Thr176. By contrast, the second amino group forms hydrogen bonds with three ordered waters (W_F, W_G, W_H), which in turn hydrogen-bond to the acidic residues Glu15, Glu178, and Glu256, and to Ser113. In addition, the carbon chain of putrescine forms hydrophobic interactions with the aromatic residues Phe111, Phe285, and Tyr318. The putrescine binding site is well separated (15−20 Å) from the cleavage site.

The third difference compared to the structure of fully processed AdoMetDC is the presence of a bound Tris molecule. A patch of well-formed electron density near the entrance to the active site was determined to correspond to the buffer molecule Tris (Figure 5). A reexamination of the mature AdoMetDC indicated that Tris was bound in that structure as well, but these data were interpreted as water molecules in the lower resolution electron density maps (*3*). The Tris amino group hydrogen-bonds to the backbone carbonyl oxygen of Cys226 and to two water molecules, while the Tris hydroxyl groups form hydrogen bonds to both of the side chain oxygens of Glu247, to several water molecules, and weakly to the $N^{\epsilon 2}$ of His5. Moreover, the nonpolar atoms of Tris appear to nestle against the aromatic ring of Phe7, forming a stabilizing hydrophobic interaction. Analogous hydrogen bonding interactions with Glu247 and hydrophobic interactions with Phe7 have been observed in

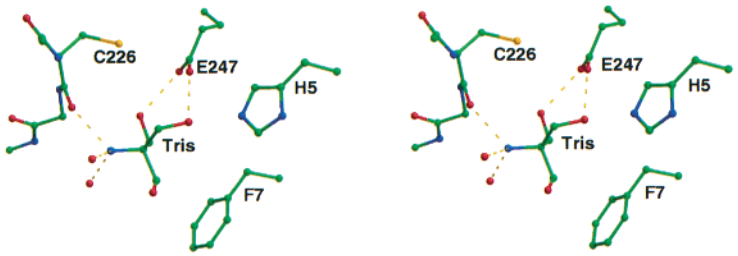

FIGURE 5: Stereoview of a ball-and-stick model of the Tris binding site. Key residues are shown with hydrogen bonds indicated by dashed lines.

five recently determined AdoMetDC/inhibitor complexes (*4*). The binding of Tris serves to partially block entry to the active site, and Tris-mediated competitive inhibition of the enzyme was observed in early studies of AdoMetDC activity (*13*, *30*). Nevertheless, crystal structures with inhibitors have been recently obtained in Tris buffer (*4*) showing that the Tris can be relatively easily displaced by tight-binding ligands.

Stimulation of Processing of AdoMetDC Proenzyme Mutants by Diamines. The observation of putrescine in the H243A AdoMetDC identified interactions with several charged amino acid residues and suggested additional kinetic studies of putrescine stimulation of AdoMetDC self-processing. Maximal stimulation of the processing rate of the AdoMetDC proenzyme is produced by putrescine, but a lesser stimulation occurs in response to several other diamines containing three, five, six, or seven carbon atoms (Figure 6A). Processing was also stimulated by 4-aminobutanol (Figure 6B) but not by 1,4-butanediol, 4-aminobutyric acid, tetramethyl-1,4-butanediamine, tetramethylammonium iodide, and ammonium chloride even at millimolar concentrations (results not shown). Much higher concentrations of 4-aminobutanol (30 mM) were needed to get a maximal rate of AdoMetDC proenzyme processing than of putrescine (0.5 mM). The apparent dissociation constant, K_d, for the stimulation of processing by putrescine is about 0.05 mM, and the equivalent K_d for 4-aminobutanol was 3.8 ± 2 mM. The maximal processing rate of AdoMetDC with 4-aminobutanol was 2.7% per minute compared to 3.9% per minute for putrescine.

The self-processing of the acid-to-amide E11Q, D174N, E178Q, and E256Q mutants is not stimulated significantly by putrescine (*7*, *11*, *29*) (Figure 6C). By contrast, 4-aminobutanol stimulates the self-processing of the E178Q mutant and has a slight stimulatory effect on E256Q but has no effect on the D174N and E11Q mutants (Figure 6C). This result is consistent with the concept that 4-aminobutanol can bind and bring about a similar change in AdoMetDC structure to putrescine, most likely with the amino group oriented toward Asp174 and the hydroxyl group interacting with Glu178 and Glu256.

Conservative mutations of four acidic residues needed for putrescine activation were made by changing them individually or in pairs to the other acidic amino acid, and the effect of diamines and 4-aminobutanol on the proenzyme processing rate was examined (Figure 7 and Table 2). Any one of the four single mutations significantly slowed the processing rate (Table 2). Mutant E178D was activated by both putrescine and 4-aminobutanol, but, in contrast to the results with wild-type AdoMetDC (Figure 6B), 4-aminobutanol was more effective with this mutant (Figure 6A). Processing of the proenzyme from mutant D174E was stimulated by

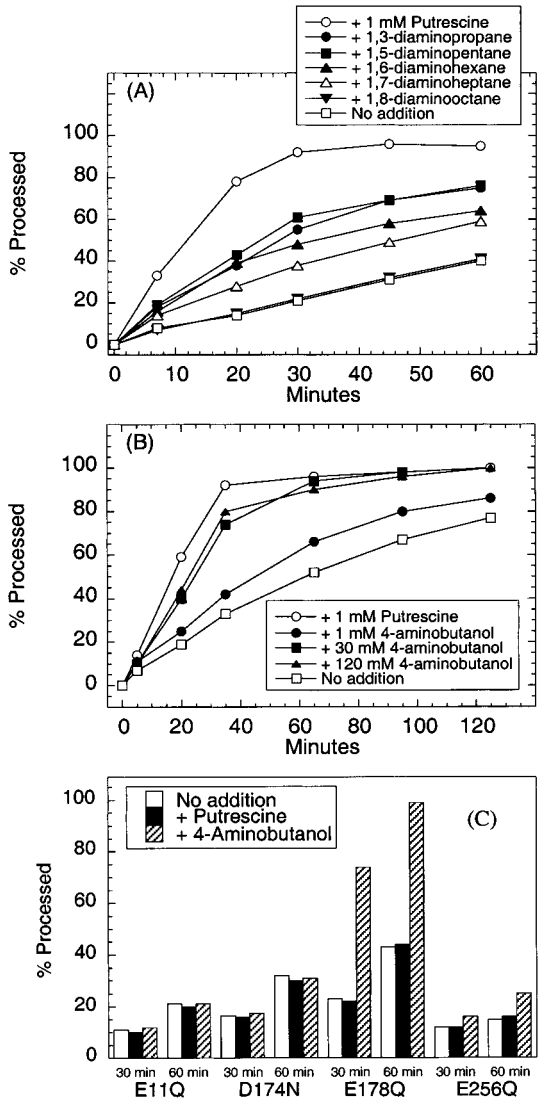

FIGURE 6: Processing of AdoMetDC proenzyme in the presence of various diamines and 4-aminobutanol. Human AdoMetDC proenzyme was synthesized in a TNT reaction from the pCM9 plasmid. After the 30 min synthesis, a 1 mM aliquot of putrescine (1,4-diaminobutane) or the other diamines indicated was added to the reactions, and the processing was measured over the next 60 min. Panel (A) shows the effects of various diamines as indicated. Panel (B) shows the results of adding putrescine or 4-aminobutanol at the concentration indicated. Panel (C) shows the effects of either 1 mM putrescine or 60 mM 4-aminobutanol on the processing of AdoMetDC proenzyme mutants E11Q, D174N, E178Q, and E256Q in the presence of 1 mM putrescine or 60 mM 4-aminobutanol or of no addition as indicated after either 30 or 60 min.

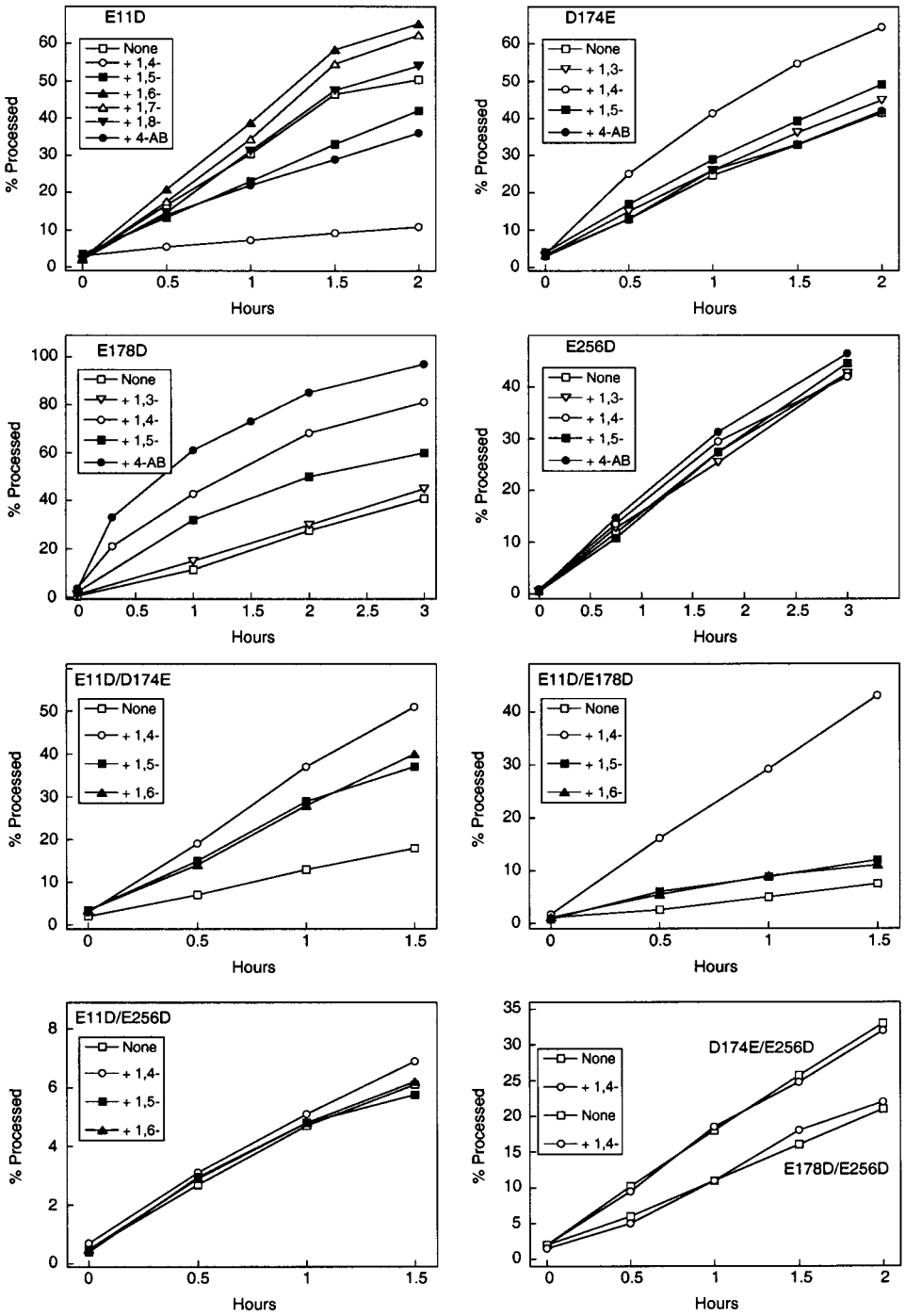

FIGURE 7: Effect of diamines and 4-aminobutanol on the processing of AdoMetDC proenzyme with mutations at conserved acidic residues. The processing of the single mutant AdoMetDCs E11D, D174E, E178D, and E256D and the double mutants E11D/D174E, E11D/E1786D, E11D/E256D, D174E/E256D, and E178D/E256D in the presence of a 1 mM aliquot of the diamines indicated (shown as 1,3-, 1,4-, etc.) or 60 mM 4-aminobutanol (4-AB) or no addition as indicated was measured as described in the legend to Figure 6 and plotted as the extent of processing against time.

putrescine but not by 4-aminobutanol. Processing of the proenzyme from mutant E256D was not stimulated by any of the amines tested and only very slightly by 4-aminobutanol. 1,3-Diaminopropane did not stimulate processing of any of these mutant AdoMetDC proenzymes.

The E11D mutation produced a most striking difference in the response of the AdoMetDC proenzyme to diamines (compare Figure 6A to Figure 7). Instead of the stimulation seen with wild-type AdoMetDC, putrescine was a potent *inhibitor* of the processing of mutant E11D (Table 2), while cadaverine (1,5-diaminobutane) and 4-aminobutanol also had clear (but weaker) inhibitory effects (Figure 7). Longer diamines (1,6-diaminohexane and 1,7-diaminoheptane) weakly stimulated processing of this mutant in a similar way to their effect on wild type.

The strong inhibition of processing produced by putrescine with the E11D mutant was abolished when this mutation was combined with any one of the other three mutations. Combination with D174E or with E178D actually restored stimulation by putrescine (Figure 7 and Table 2), and the E11D/D174E mutant also showed substantial activation by other diamines. However, even in the presence of putrescine,

Table 2: Effect of Conservative Mutations on Processing of AdoMetDC Proenzyme

mutant	rate of processing (%/min)	
	+putrescine	−putrescine
wild type	3.9	0.8
E11D	0.07	0.6
D174E	0.7	0.4
E178D	0.7	0.2
E256D	0.2	0.2
E11D/D174E	0.7	0.2
E11D/E178D	0.8	0.1
E11D/E256D	0.09	0.08
D174E/E256D	0.25	0.25
E178D/E256D	0.16	0.16

the overall processing rates of E11D/D174E and E11D/E178D were still much slower than that of wild-type enzyme (Table 2). Processing of the double mutant E11D/E256D was extremely slow (Figure 7, note scale), and none of the diamines tested including putrescine had any effect on the processing. There was also no effect of any diamine on the processing of double mutants D174E/E256D and E178D/E256D that each processed at about the same rate as E256D.

DISCUSSION

Trapping of the Ester Intermediate in H243A AdoMetDC. An ester intermediate has long been considered the most plausible pathway for self-cleavage in pyruvoyl enzymes (*2*) and is supported by several biochemical, radioactive labeling, and site-directed mutagenesis experiments (*31*). Structural evidence for the ester intermediate in pyruvoyl-enzyme processing was previously reported in the structure of aspartate decarboxylase (AspDC) (*6*). Biochemical experiments had suggested that only three pyruvoyl groups are present in this tetrameric enzyme, indicating incomplete processing for the fourth subunit. In the X-ray crystal structure of AspDC, the amide form of the proenzyme did not fit well into the electron density of this fourth subunit, giving several local Ramachandran outliers and some distortion of the planarity of the Gly24−Ser25 peptide bond. By contrast, the ester intermediate produced a better fit to the electron density (lower *R*-free value). However, the ester bond could not be discerned clearly, since this region of the electron density was largely disordered, with most atomic *B*-factors in adjacent residues between 45 and 65 Å^2. The higher resolution and lower *B*-factors (7−20 Å^2) of the corresponding region in the AdoMetDC H243A mutant allow the amide form of the Glu67−Ser68 peptide bond to be ruled out definitively, and provide the first clearly resolved structure of an ester intermediate of the self-processing reaction.

In contrast to AspDC, the ester linkage in H243A AdoMetDC is well-defined. An ester linkage between amino acid residues is generally unstable at neutral pH and converts rapidly to the more stable amide linkage in model systems (*32*). The ester intermediate is trapped by the H243A mutant of AdoMetDC, indicating that the enzyme is unable to progress to the next step in the processing reaction (β-elimination) and that the rate of back-conversion to the amide is negligible. The β-elimination step likely involves an initial abstraction of the H$^\alpha$ proton of residue 68 with the resulting negative charge delocalized over the adjacent amide bond. The negative charge would be further stabilized by protonation of the amide carbonyl. Because the ester is trapped in the H243A mutant, the side chain of His243 is a strong candidate as the base involved in H$^\alpha$ proton extraction. The position of the His243 side chain modeled into the His243 ester structure shows that the N$^{\epsilon 2}$ atom is near the H$^\alpha$ proton (Figure 3B). Interestingly, this orientation of the His243 side chain places N$^{\delta 1}$ near the Glu11 side chain, possible forming a catalytic triad, consistent with mutational studies of Glu11 that indicate a key role for this amino acid side chain. In the ester intermediate structure, there is no residue near the carbonyl group of residue 68, suggesting that the base alone is sufficient for abstraction of the H$^\alpha$ proton.

The back-conversion to the more stable amide form of the peptide bond might be prevented by several factors. Protonation of the displaced amino group (*32*) would result in a less active nucleophile. This amino group is hydrogen-bonded to three ordered water molecules (W_A, W_C, and W_D); however, this arrangement is consistent with either a protonated or a deprotonated amino group. Even if the displaced amino group is not protonated, its lone-pair is unavailable for nucleophilic attack because of the hydrogen bond to the third water molecule. In effect, a "desolvation penalty" must be paid before the amino group can be made reactive. The back-reaction to the amide form of the peptide bond may also be inhibited by holding the reactive amino and carbonyl groups apart. The amino group and the ester carbonyl in H243A AdoMetDC are on opposite sides of the ester linkage with no obvious path for nucleophilic attack. These groups appear to be part of a rigid structural unit with low thermal *B*-factors (near 15−20 Å^2) suggesting that the connecting ester atoms are unlikely to undergo large motions.

The oxygen atoms of the ester bond do not appear to be involved in hydrogen bonds. The backbone carbonyl oxygen of Glu67 is sequestered in an amphipathic pocket, and is surrounded by Cys49, Cys82, and the hydrophobic atoms of Thr81 and Thr85. The closest potential hydrogen bond partner (the backbone nitrogen of Cys82) is separated from this carbonyl oxygen by 3.39 Å. A water molecule could possibly bind in this pocket, forming hydrogen bonds to the backbone atoms of Cys82, the carbonyl oxygen of Glu67, and also the side chains of Thr85 and Glu67. However, no such water molecule is observed in the electron density. Thus, there appears to be no "oxyanion hole" stabilizing the carbonyl group of the scissile peptide bond, contrary to the situation in serine proteases (*33*) and the GyrA intein (*34*).

Implications for the Mechanism of Self-Processing in Wild-Type AdoMetDC. The first step of the self-processing reaction is attack by the Ser68 side chain of the adjacent carbonyl carbon atom of Glu67. It is generally believed that Ser68 must be activated for its nucleophilic attack by the abstraction of the proton from its side chain oxygen by a nearby basic residue. The structure of the H243A ester intermediate should be structurally more similar to the proenzyme than is the fully processed AdoMetDC. However, in the H243A model, there is no obvious base near the Ser68 side chain and no obvious acid near the carbonyl group of Glu67. The side chain of Ser68 is relatively close to Glu11 and Cys82, but their side chain atoms seem too distant to act as proton acceptors unless they act through ordered water molecules. Moreover, mutations of these two residues generally do not

affect processing, only the putrescine stimulation of processing. The sole exception is the charge-reversing E11K mutation, which eliminates processing altogether (*29*). Other, more distant candidates include Glu67 and His243, but these residues are excluded by site-directed mutagenesis data (*8, 11*). This suggests that the proenzyme structure must be significantly different from that of either the fully processed or the H243A mutant AdoMetDCs. It has been suggested that in HisDC the amide form of the proenzyme is under considerable strain that is relieved only after the transition to the ester intermediate (*2*). The strain hypothesis is also supported by observations of unusual cis nonprolyl peptide bonds (*34*) and nonplanar peptide bonds (*35*) in noncleaving mutant analogues of self-processing enzymes. Structural evidence for strain in the proenzyme might be provided by the structure of the S68A mutant, which lacks the serine side chain and does not process at all. Thus far, we have been unable to crystallize the S68A mutant of AdoMetDC.

After the N→O acyl shift, the next step in AdoMetDC processing is a β-elimination, in which the H^{α} proton of residue 68 is abstracted to cleave the peptide chain and form the dehydroalanine residue. The proton abstraction may be a rate-determining step of pyruvoyl-enzyme processing, judging from the hydrogen−deuterium isotope effect (1.6) observed in HisDC with α-deuterated serine (*36*). As discussed above, the H243A side chain is the most likely candidate for the proton abstraction. Furthermore, it appears that the C−H bond is aligned with the carbonyl bond as would be expected for an E1 mechanism. His243 may also play a role in the protonation either of the dehydroalanine methylene carbon atom or of the displaced amino group, as would be required for release of ammonia after hydrolysis. By rotation about the $C^{\alpha}-C^{\beta}$ bond, His243 can be positioned to serve as the proton donor for either of these functional groups (Figure 3B). Consistent with mutagenesis data (*19*), the side chains of the adjacent residues Ser66, Glu67, and Ser69 do not appear to interact with the atoms involved in the processing or β-elimination reactions.

Mechanism for Putrescine Simulation of AdoMetDC Proenzyme Processing. The effects of putrescine are small (about an 5−8-fold increase in rate of processing) but reproducible, and the effects are modulated by mutation of certain amino acid side chains. The structure of H243A AdoMetDC with bound putrescine suggests that the effect must be exerted indrectly because the putrescine binding site is separated from the active site by about 15−20 Å. Only one bound putrescine molecule is observed per monomer, contrary to an earlier hypothesis (*9, 37*) that two putrescine molecules would bind to each monomer. The presence of putrescine in the H243A structure was somewhat surprising because no putrescine was added during crystallization. However, putrescine is present at high concentration in the *E. coli* expression system and was also present in the buffers during purification. Because the putrescine binding site is buried, the release of bound putrescine may occur slowly. It is possible that a second low-affinity site exists but is unoccupied. Although this possibility cannot be eliminated, all of the site-directed mutagnesis and kinetic data related to putrescine activation are consistent with a single-site model.

In principle, putrescine could exert its effects through conformational changes, electrostatic effects, or both. The kinetic data are generally consistent with a model in which binding of putrescine or 4-aminobutanol to AdoMetDC proenzyme occurs via interactions with acidic residues, Glu178, Glu256, and Asp174, at a remote site, thus altering the positioning or properties of Glu11. The inhibitory effect of the E11D mutation on processing after binding of putrescine may be attributed to the mispositioning of the side chain carboxylate group of Asp11 (by ∼1.5 Å) in the active putrescine-bound conformation. Presumably, the D174E and E178D mutations alter this conformation enough to prevent Asp11 from interfering with processing.

Putrescine may act in part by stabilizing the proper association of the two layers of the β-sandwich. Such structural stabilization could aid in the self-cleavage reaction by bringing the required functional groups (e.g., Glu11, Ser68, Cys82, Ser229, and His243) from each β-sheet into their proper positions. As described above, putrescine forms specific hydrogen bonds and hydrophobic packing interactions with residues of both β-sheets, and its positive charges may help to neutralize the negatively charged groups occupying the core of the β-sandwich, such as Glu15, Asp174, Glu178, and Glu256.

A second effect of putrescine that appears to further assist the self-processing reaction is likely to occur through specific effects on the active site residues Lys80 and Glu11. These effects are transmitted through a chain of hydrogen bonds linking these residues to the putrescine binding site. Glu11 appears to play an important role in the β-elimination step of processing by assisting the deprotonation of the α-carbon by His243. Glu11 is linked to the putrescine binding site through its interaction with the side chain amino group of the conserved residue Lys80. The amino group of Lys80 is positioned loosely between three acidic residues (Glu11, Glu178, and Glu256). The electron density for this lysine is poorly resolved, indicating possible disorder and multiple transient associations with the surrounding acidic groups. The binding of putrescine might affect the position of Lys80 through its interactions with Glu178 and Glu256. Thus, putrescine binding may cause a shift in the position of Glu11, promoting the proton abstraction required for β-elimination.

This mechanism is consistent with the mutagenesis data. The E11Q mutant processes more slowly than the wild-type proenzyme, and its processing is not stimulated by putrescine [Figure 6C and (*29*)]. Similarly, the mutation of Lys80 to Ala slows the processing reaction 5-fold and abolishes stimulation by 0.2 mM putrescine (*11*), even though its side chain amino group is also distant from the bound putrescine. Lys80 is not a conserved residue in AdoMetDCs; for example, this position is occupied by Ile in AdoMetDC from *T. cruz*i. However, although the *T. cruzi* AdoMetDC is putrescine-activated, its proenzyme processing is not stimulated by putrescine (unpublished observations). There are other experimental indications showing that although putrescine increases the activity of human AdoMetDC and enhances the processing rate of the proenzyme, these effects are not identical (*9*). Furthermore, although 4-aminobutanol simulates processing, it did not stimulate the enzymatic activity of human AdoMetDC even at 120 mM. By contrast, 1 mM putrescine stimulated the enzymatic activity by a factor of about 3.5 with an apparent activation constant of 4.5 μM (results not shown). These data are therefore consistent with a mechanism for putrescine activation in which one pu-

trescine molecule per monomer exerts its effect indirectly through Glu11.

ACKNOWLEDGMENT

We thank the Structural Biology Center of the Advanced Photon Source for providing synchrotron beam time. We thank Ms. Leslie Kinsland for preparation of figures and for assistance in the preparation of the manuscript.

REFERENCES

1. Hackert, M. L., and Pegg, A. E. (1997) in *Comprehensive Biological Catalysis* (Sinnott, M. L., Ed.) pp 201−216, Academic Press, London.
2. van Poelje, P. D., and Snell, E. E. (1990) *Annu. Rev. Biochem. 59*, 29−59.
3. Ekstrom, J. E., Matthews, I. I., Stanley, B. A., Pegg, A. E., and Ealick, S. E. (1999) *Structure 7*, 583−595.
4. Tolbert, W. D., Ekstrom, J. L., Mathews, I. I., Secrist, J. A., III, and Kapoor, P. (2001) *Biochemistry 40*, 9484−9494.
5. Gallagher, T., Rozwarski, D. A., Ernst, S. R., and Hackert, M. L. (1993) *J. Mol. Biol. 230*, 516−528.
6. Albert, A., Dhanaraj, V., Genschel, U., Khan, G., Ramjee, M. K., Pulido, R., Sibanda, B. L., von Delft, F., Witty, M., Blundell, T. L., Smith, A. G., and Abell, C. (1998) *Nat. Struct. Biol. 5*, 289−293.
7. Xiong, H., Stanley, B. A., Tekwani, B. L., and Pegg, A. E. (1997) *J. Biol. Chem. 272*, 28342−28348.
8. Xiong, H., and Pegg, A. E. (1999) *J. Biol. Chem. 274*, 35059−35066.
9. Stanley, B. A. (1995) in *Polyamines: Regulation and Molecular Interaction* (Casero, R. A., Ed.) pp 27−75, R. G. Landes Co., Austin, TX.
10. Kameji, T., and Pegg, A. E. (1987) *Biochem. J. 243*, 285−288.
11. Stanley, B. A., and Pegg, A. E. (1991) *J. Biol. Chem. 266*, 18502−18506.
12. Tabor, C. W., and Tabor, H. (1984) *Adv. Enzymol. Related Areas Mol. Biol. 56*, 251−282.
13. Pegg, A. E., and Williams-Ashman, H. G. (1969) *J. Biol. Chem. 244*, 682−693.
14. Hoyt, M. A., Williams-Abbott, L. J., Pitkin, J. W., and Davis, R. H. (2000) *Mol. Gen. Genet. 263*, 664−673.
15. Persson, K., Aslund, L., Grahn, B., Hanke, J., and Heby, O. (1998) *Biochem. J. 333*, 527−537.
16. Tekwani, B. L., Bacchi, C. J., and Pegg, A. E. (1992) *Mol. Cell. Biochem. 117*, 53−61.
17. Perler, F. B., Xu, M. Q., and Paulus, H. (1997) *Curr. Opin. Chem. Biol. 1*, 292−299.
18. Teixeira, M. T., Fabre, E., and Dujon, B. (1999) *J. Biol. Chem. 274*, 32439−32444.
19. Stanley, B. A., Pegg, A. E., and Holm, I. (1989) *J. Biol. Chem. 264*, 21073−21079.
20. Shantz, L. M., Stanley, B. A., Secrist, J. A., and Pegg, A. E. (1992) *Biochemistry 31*, 6848−6855.
21. Otwinowski, Z., and Minor, W. (1997) *Methods Enzymol. 276*, 307−326.
22. Brünger, A. T., Adams, P. D., Clore, G. M., DeLano, W. L., Gros, P., Grosse-Kunstleve, R. W., Jiang, J. S., Kuszewski, J., Nilges, M., Pannu, N. S., Read, R. J., Rice, L. M., Simonson, T., and Warren, G. L. (1998) *Acta Crystallogr., Sect. D D54*, 905−921.
23. Brünger, A. T. (1992) *Nature 355*, 472−475.
24. (2000) Tripos Inc., St. Louis, MO.
25. Jones, T. A., Zou, J.-Y., Cowan, S. W., and Kjeldgaard, M. (1991) *Acta Crystallogr., Sect. A A47*, 110−119.
26. Kleywegt, G. J. (1995) *CCCP4/ESF-EACBM Newslett. Protein Crystallogr. 31*, 45−50.
27. Laskowski, R. A., MacArthur, M. W., Moss, D. S., and Thornton, J. M. (1993) *J. Appl. Crystallogr. 26*, 283−291.
28. Ramachandran, S. (1968) *Adv. Protein Chem. 23*, 283−437.
29. Stanley, B. A., Shantz, L. M., and Pegg, A. E. (1994) *J. Biol. Chem. 269*, 7901−7907.
30. Zappia, V., Carteni-Farina, M., and Della Pietra, G. (1972) *Biochem. J. 129*, 703−709.
31. Recsei, P. A., and Snell, E. E. (1985) *J. Biol. Chem. 260*, 2804−2806.
32. Iwai, K., and Ando, T. (1967) *Methods Enzymol. 11*, 263−282.
33. Fersht, A. R. (1999) *Structure and Mechanism in Protein Science*, W. H. Freeman, New York.
34. Klabunde, T., Sharma, S., Telenti, A., Jacobs, W. R., and Sacchettini, J. C. (1998) *Nat. Struct. Biol. 5*, 31−36.
35. Xu, Q., Buckley, D., Guan, C., and Guo, H.-C. (1999) *Cell 98*, 651−661.
36. Recsei, P., and Snell, E. (1984) *Annu. Rev. Biochem. 53*, 357−387.
37. Dezeure, F., Gerhart, F., and Seiler, N. (1989) *Int. J. Biochem. 21*, 889−899.
38. Esnouf, R. (1997) *J. Mol. Graphics 15*, 132−134.
39. Esnouf, R. M. (1999) *Acta Crystallogr., Sect. D D55*, 938−940.
40. Merritt, E. A., and Bacon, D. J. (1997) *Methods Enzymol. 277*, 505−524.

BI010736O